Color changing photonic crystals detect blast exposure

D. Kacy Cullen [a], Yongan Xu [b], Dexter V. Reneer [c], Kevin D. Browne [a], James W. Geddes [c], Shu Yang [b,*], Douglas H. Smith [a,*]

[a] Center for Brain Injury and Repair, Dept. of Neurosurgery, School of Medicine, University of Pennsylvania, 105 Hayden Hall, 3320 Smith Walk, Philadelphia, PA 19104, USA
[b] Dept. of Materials Science and Engineering, School of Engineering and Applied Science, University of Pennsylvania, 3231 Walnut Street, Philadelphia, PA 19104, USA
[c] Spinal Cord and Brain Injury Research Center, Dept. of Anatomy and Neurobiology, College of Medicine, University of Kentucky, Chandler Medical Center, B477 Biomed & Biol Science Research Bldg, 741S. Limestone St., Lexington, KY 40536, USA

ARTICLE INFO

ABSTRACT

Blast-induced traumatic brain injury (bTBI) is the "signature wound" of the current wars in Iraq and Afghanistan. However, with no objective information of relative blast exposure, warfighters with bTBI may not receive appropriate medical care and are at risk of being returned to the battlefield. Accordingly, we have created a colorimetric blast injury dosimeter (BID) that exploits material failure of photonic crystals to detect blast exposure. Appearing like a colored sticker, the BID is fabricated in photosensitive polymers via multi-beam interference lithography. Although very stable in the presence of heat, cold or physical impact, sculpted micro- and nano-structures of the BID are physically altered in a precise manner by blast exposure, resulting in color changes that correspond with blast intensity. This approach offers a lightweight, power-free sensor that can be readily interpreted by the naked eye. Importantly, with future refinement this technology may be deployed to identify soldiers exposed to blast at levels suggested to be supra-threshold for non-impact blast-induced mild TBI.

Introduction

Blast-induced traumatic brain injury (bTBI) is a major source of battlefield morbidity in the current wars in Iraq and Afghanistan (Okie, 2005; Warden et al., 2005; Taber et al., 2006; Warden, 2006). This reflects a stunning number of warfighters who have been exposed to blast shockwave, typically from improvised explosive devices (IEDs). However, little is known about blast exposure thresholds that induce bTBI. Indeed, many warfighters who display either no overt symptoms or only minor cognitive deficits after blast exposure may nonetheless have suffered brain damage (Ling, 2008). With no objective information of relative blast exposure, warfighters with bTBI may not receive appropriate acute or chronic care. Furthermore, if returned to service, they may be at risk of an exacerbated response with repetitive blast exposure, as is the case in repetitive head injury in sports (Guskiewicz et al., 2003; Mori et al., 2006). Accordingly, there is a critical need for a wearable sensor capable of registering the severity of blast exposure in relation to the risk of bTBI.

To address these needs, our objective is to utilize a material-based strategy that directly exploits blast energy to induce optical changes in photonic crystalline microstructures. The level of blast exposure would then be observed based on a visible color change. This technology may be used to develop a small wearable blast injury dosimeter (BID) to readily designate soldiers exposed to blast conditions associated with TBI and other injuries (patent pending). For this application, we utilized 3-D photonic crystalline microstructures that were fabricated via multi-beam interference lithography (MBIL) of a commercially available, negative-tone photoresist, SU-8, using a visible ($\lambda = 532$ nm) laser (Campbell et al., 2000; Yang et al., 2002; Miklyaev et al., 2003; Moon and Yang, 2005; Xu et al., 2008). SU-8 is a bisphenol-A novolac resin derivative with an average of eight epoxy groups per chain. SU-8 is highly soluble in many organic solvents, enabling preparation of ultra-thick films (up to 2 mm) that are highly transparent in the near-UV and visible region. SU-8 has been widely used in microelectromechanical systems (MEMS) (Lorenz et al., 1997), microfluidics (Ribeiro et al., 2005), high-aspect ratio (≥ 20) microstructures (Lee et al., 1994), and 3-D photonic structures (Campbell et al., 2000; Yang et al., 2002; Miklyaev et al., 2003; Moon et al., 2006). Crystalline films made from SU-8 create a colorful reflection due to the diffraction grating of the underlying pattern, which is a characteristic of the periodicity (~ 1 μm) and refractive index contrast between high (SU-8, $n = 1.6$) and low (air, $n = 1$) dielectric materials, and the viewing angle. Importantly, the SU-8 photonic crystals are thermally stable up to 300 °C and chemically inert due to aromatic functionality and high cross-link density. Thus, they are highly durable under extreme weather conditions (e.g., heat, cold, and

* Corresponding authors. D.H. Smith is to be contacted at Dept. of Neurosurgery, University of Pennsylvania, 105 Hayden Hall, 3320 Smith Walk, Philadelphia, PA 19104, USA. Fax: +1 215 573 3808. Yang, Dept. of Materials Science and Engineering, University of Pennsylvania, 3231 Walnut Street, 203 LRSM, Philadelphia, PA 19104, USA. Fax: +1 215 573 2128.
E-mail addresses: shuyang@seas.upenn.edu (S. Yang), smithdou@mail.med.upenn.edu (D.H. Smith).

moisture) or physical impact associated with combat situations. Moreover, the small, lightweight design can easily be accommodated across multiple locations on and in helmets and uniforms, thus rendering the BID useful for in-field interpretation (Fig. 1).

The objective of the current study was to establish proof-of-principle data that our photonic crystalline microstructures respond specifically to blast exposure. In particular, we assessed colorimetric changes in custom-engineered photonic crystals based on dynamic overpressure exposure, and correlated this color change with ultrastructural alterations and damage. This demonstration is necessary to enable the ultimate application of this device as a means to measure single or cumulative blast exposure supra-threshold for bTBI. Thus, future studies will directly calibrate these color changes to potentially unique blast-induced neuropathology to fulfill our objective for a material-based colorimetric blast injury dosimeter.

Methods

Photonic crystal fabrication

Diamond-like photonic crystals consisting of periodic arrangement of polymer and air voids were fabricated from the negative photoresist, SU-8, by MBIL using the same optical setup reported earlier (Xu et al., 2008). Briefly, SU-8 film was exposed to four umbrella-like visible laser beams split from one coherent laser source ($\lambda = 532$ nm, power diode-pumped Nd:YVO4 laser). The central beam was circularly polarized and incident perpendicularly to the photoresist film. The other three beams were polarized linearly in a plane formed by the wave vectors of the central beam and surrounding beam. The wave vector of each beam was $k_0 = \pi/a[3\ 3\ 3]$, $k_1 = \pi/a[5\ 1\ 1]$, $k_2 = \pi/a[15\ 1]$, and $k_3 = \pi/a[1\ 1\ 5]$, respectively. The polarization vectors of beam 1, 2, and 3 were $e_1 = [-0.272\ 0.680\ 0.680]$, $e_2 = [0.680 - 0.272\ 0.680]$, and $e_3 = [0.680\ 0.680 - 0.272]$, respectively. The intensity ratio was 1.8:1:1:1. The circular polarization of the central beam distributes the intensity equally to the surrounding beams.
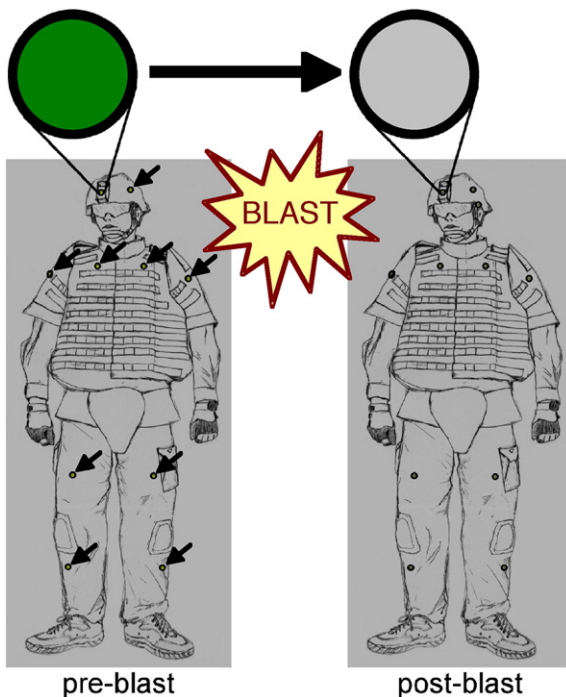
Fig. 1. Blast injury dosimeter (BID) concept. BIDs exhibiting pre-characterized colorimetric properties may be attached to soldiers' uniforms in several locations (small arrows) (left). Blast exposure disrupts the BID nanostructure, resulting in clear colorimetric changes (right). The color change may be calibrated to denote the severity of blast exposure in relation to thresholds for bTBI.

The photoresist was prepared by mixing Epon SU-8 pellets and 2.0 wt.% Irgacure 261 (Ciba Specialty Chemicals) as visible photo-initiators in γ-butyrolactone (Aldrich) to form 58 wt.% solution. Substrates were transparent glass or flexible aclar membranes (SPI Supplies). To ensure good adhesion with the SU-8 film, the substrate was cleaned by ultrasonication in isopropanol and acetone, respectively, followed by oxygen plasma. The photoresist solution was spin-coated on the substrate at 2000 rpm for 30 s, followed by pre-exposure bake at 65 °C for 3 min and 95 °C for 40 min, respectively, resulting in a film thickness of ~6 μm. The film was exposed to the superimposed interference beams (laser output of 1 W) for 1–2 s. After post-exposure bake at 65 °C for 2–4 min and 95 °C for 2–4 min, respectively, the exposed film was developed in propylene glycol monomethyl ether acetate (Aldrich) to remove unexposed or weakly exposed films, resulting in 3-D microporous structures. To prevent the pattern collapse of the 3-D porous film during air-drying, the film was dried using a supercritical CO_2 dryer (SAMDRI®-PVT-3D; Tousimis) after the development.

Colorimetric properties

Photonic crystalline colorimetric properties are an inherent consequence of the periodic modulation of refractive index arranged in 3-D, where interference of the light waves leads to stop bands or photonic band gaps. This results in light of a particular range of wavelength being totally reflected in a photonic crystal. Briefly, when light arrives at the surface of the periodic structures, it is strongly reflected by constructive interference between reflections from the different interfaces of a stack of thin films (thickness of d) of alternately high and low refractive index (n), resulting in so-called structural color. According to Bragg's Law, at the normal incidence to the (111) plane the reflectance peak wavelength is

$$\lambda = 2d_{111}n_{\text{eff}} \tag{1}$$

where d_{111} is the interlayer distance in the [111] direction, and n_{eff} is the effective refractive index of the film:

$$n_{\text{eff}}^2 = f_1 n_1^2 + (1-f_1)n_2^2 \tag{2}$$

where n_1 and n_2 are the refractive index of components 1 and 2, respectively, and f_1 is the filling volume fraction of component 1. Here, $n_{\text{SU-8}} = 1.6$ and $n_{\text{air}} = 1$.

BID testing

For design feedback, we evaluated the structural/colorimetric alterations of the photonic crystalline microstructures following exposure to surrogate blast conditions from (1) targeted blast-like overpressure from single-pulse ultrasonic irradiation, or (2) blast from an explosive-based shocktube.

Single-pulse ultrasonic irradiation. Blast-like overpressure exposure was generated using a modified piezoelectric transducer to generate a rapid, single pulse (100–200 ms in duration) applied focally using a sonication wand (Fisher Scientific Model 100 Sonic Dismembrator). This employed locally applied stress waves to approximate the effects of a globally applied blast wave. This process generated extremely rapid pressure fluctuations that approximate some facets of blast exposure; specifically, both may exhibit extreme overpressure magnitudes (up to 1–10 MPa) with rapid pressure change rise-times on the order of ten microseconds. The exposure intensity was based on the power output from the device and ranged from 800 W/m² to 8000 kW/m².

Explosive-driven shocktube. The shocktube was cylindrical (21″ L×6.5″ ID) with a concave enclosure at one end. The explosive material was a gaseous mixture of hydrogen and oxygen generated in a controlled quantity by the electrolysis of H_2O (based on the time and amperage). The explosion was initiated by firing a small cordite charge into the collected gases, the quantity of which determined the magnitude of the blast conditions (e.g., peak overpressure). For each experiment, high frequency pressure transducers (500 kHz sampling rate; PCB Piezotronics) positioned immediately adjacent to BID arrays measured the local blast parameters (pressure–time functions) face-on. Each sensor was connected via coaxial cable to a PCB signal conditioner (482A21), and then to a digital oscilloscope (DSO-2250, 100 MHz bandwidth, 250 MS/s real-time sampling) and computer. The sensor voltage was converted into pressure based on the sensor-specific calibration. Following these exposures to dynamic overpressure fluctuations, alterations in the colorimetric properties and micro-structure were assessed.

Optical imaging. Light images were taken for each BID before and after surrogate blast or control (sham) conditions. Images were acquired by a digital camera (Sony) mounted on a stereoscope at 10× magnification (Nikon SMZ645). Colorimetric surface plots were generated using ImagePro Plus (Media Cybernetics). For these surface plots, the mean pixel intensity was calculated on a point-by-point basis and plotted on the z-axis to create a three-dimensional visualization (with x and y representing position on the BID surface) of photonic crystalline color changes due to blast exposure.

Scanning electron microscopy (SEM). SEM ultrastructural analysis was performed for each BID after surrogate blast or control conditions. High-resolution SEM images were acquired using a Strata DB235 Focused Ion Beam system (FEI) at an e-beam voltage of 5 kV. Prior to SEM analysis, the samples were sputter coated with gold (thickness <10 nm).

Results and discussion

Photonic crystal fabrication and structural/colorimetric properties

The premise behind this BID is that supra-threshold blast exposure induces physical alterations in the photonic crystalline microstructures that manifest as color changes based on the level of exposure. The BIDs are comprised of arrays of diamond-like photonic crystals with nano-scale features that reflect light in specific wavelengths across the color spectrum. These photonic crystalline microstructures were fabricated on glass or thin flexible polymer sheets (<1 cm²). Macroscopically, the BIDs resembled small colored stickers with an overall diameter ranging from 1.0 to 6.5 mm. The final engineered microstructures consisted of several one-micron thick layers (total thickness was typically 6μm) with readily observed colorimetric properties (Fig. 2).

Importantly, the top-down 3-D lithographic method we employed enables precise control of the periodic structures at the nano- and micro-scales, including symmetry, periodicity, overall porosity and pore size, and film thickness. Moreover, the response to external energy can be tailored by these 3-D structural and material properties (e.g., Young's modulus, and thermal conductivity). We exploited this flexibility in fabrication to create microstructures specifically tailored for our application of blast exposure detection. In turn, the 3-D ultrastructure determines the colorimetric properties. The key feature of the BID is to exploit blast-induced nano-scale structural alterations to create a color change relative to the severity of the blast.

BID testing using surrogate blast conditions

In order to apply these 3-D photonic crystals as a BID, we evaluated the physical alterations and corresponding color change following exposure to dynamic overpressure via (1) targeted blast-like overpressure from single-pulse ultrasonic irradiation, and (2) blast from an explosion-based shocktube. We used performance feedback to engineer BIDs that exhibited overt colorimetric alterations following blast exposure. Single-pulse ultrasonic irradiation induced differential colorimetric and structural alterations proportional to pulse peak overpressure. BIDs exhibited complete color loss across the entire surface of the material with modest material loss at the edges following exposure at an intensity of 320 kW/m² (Fig. 3A). With increased dynamic overpressure intensity to 960 kW/m², BIDs demonstrated a similar color loss across the surface but had an increase in material loss at the center and edges (Fig. 3B). Additionally, colorimetric surface plots were used to map the mean pixel intensity across the face of the samples. This technique demonstrated a precipitous depression in mean pixel intensity across the entire surface of the samples, with even more dramatic changes in regions potentially experiencing material loss (e.g., center and edges).

An explosive-driven shocktube was then utilized to refine BID responses to more realistic blast conditions. The explosion in this cylindrical shocktube was driven by ignition of a gaseous hydrogen–oxygen mixture, generating pressure–time waves that were very similar to that produced by high-energy plastic explosives (Loubeau et al., 2006; Bauman et al., 2009). This high fidelity blast shockwave consisted of microsecond-scale pressure rise-times and millisecond-scale overpressure/underpressure components. Traditionally, blast injury thresholds have been based on exposure levels inducing lung damage (e.g., peak incident pressure, time duration, and subject proximity to reflective surface); however, soldiers are now surviving more powerful explosions due to advances in body armor and rapid medical intervention (Martin et al., 2008). Moreover, blast overpressure levels inducing brain injury have varied over several orders of magnitude, and are dependent upon the method of measuring pressure (e.g., face-on versus side-on, sampling rate), reported parameters (e.g., reflected pressure, peak overpressure, or mean sustained overpressure), degree of exposure (e.g., whole body, head, or brain directly) and the sensitivity of particular outcomes (Cernak et al., 2001; Moochhala et al., 2004; Kato et al., 2007; Saljo et al., 2009). Taking these caveats into account, we established proof-of-concept performance of our BID following blast exposure with peak overpressure ranging from approximately 410 to 1090 kPa (59 to 158 psi) with mean sustained overpressure ranging from 131 to 310 kPa (19 to 45 psi) lasting approximately 1–2 ms. Following blast exposure at the lower end of this range, BIDs exhibited dramatic colorimetric changes, which, for example, consisted of red/orange hues changing to yellow or blue hues (Fig. 4). Thus, by manufacturing BID with distinct initial colorimetric and ultrastructural properties, differential blast-induced color changes may be achieved following the same exposure level. Following higher intensity blast exposure at increased peak overpressures, there were overt colorimetric changes in BIDs, in some cases complete color loss or whitening, with some degree of colorimetric/material loss at the edges (Fig. 4). Of note, the BID remained adhered to the substrate, which itself was not overtly damaged, underscoring that the photonic crystals are specifically and precisely affected by blast.

BID testing using repeat blast exposure

Since many warfighters have had multiple blast exposures, another key target of the BID technology is detection of cumulative blast exposure. Accordingly, we exposed BIDs to repeated insults, first ranging the intensity of pressure exposure over three orders of magnitude, followed by repeated exposure to a fixed intensity. Low magnitude dynamic overpressure did not result in material failure or alterations in the colorimetric properties of the BIDs. When the same
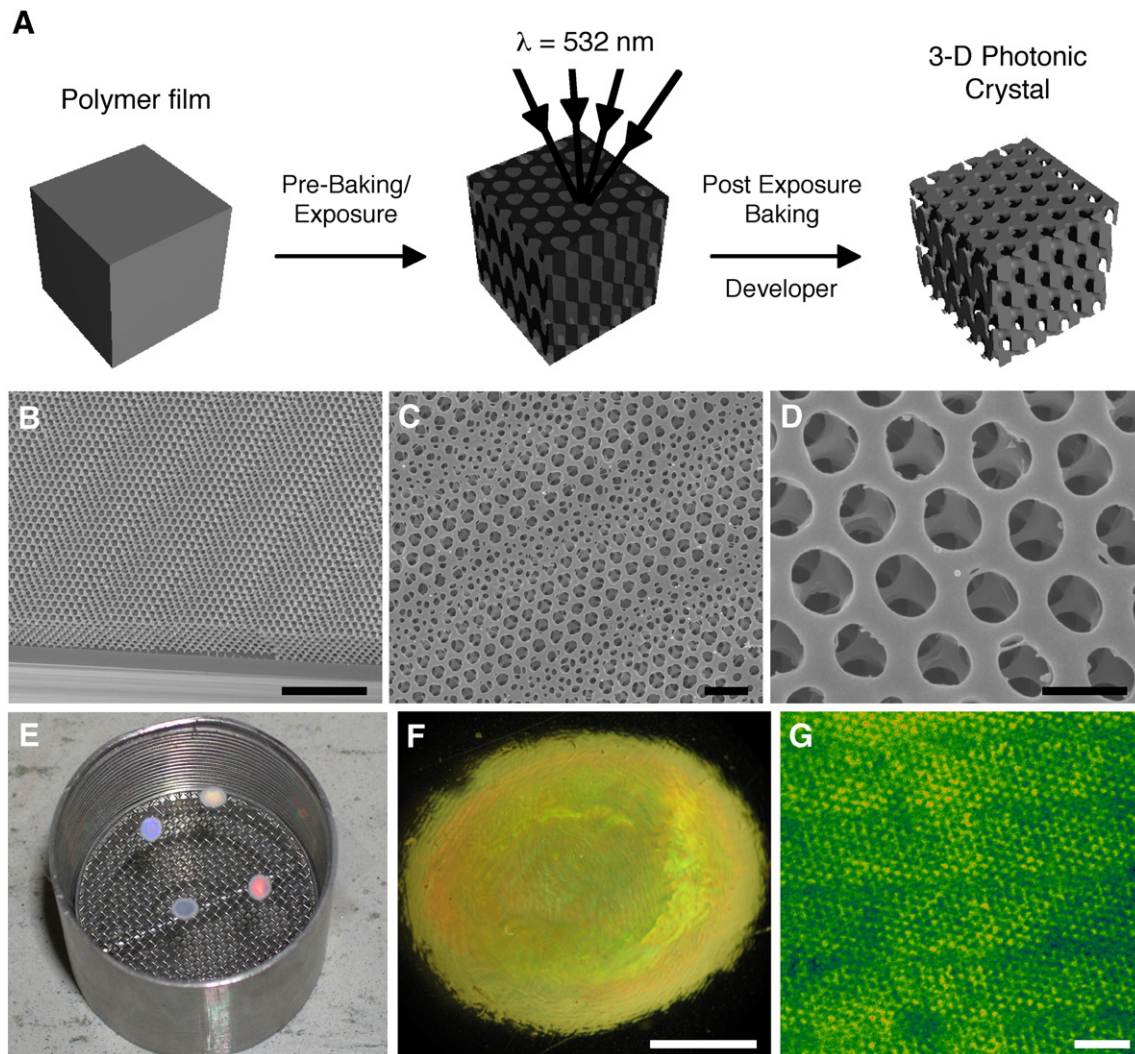
Fig. 2. BID fabrication and structural/colorimetric properties. (A) Multi-beam interference lithography (MBIL) was utilized to create the BIDs. Here, a photosensitive polymer film was exposed to an array of laser beams split from one coherent laser source ($\lambda = 532$ nm) to create the 3-D photonic crystalline microstructures. (B–D) Scanning electron micrographs demonstrating the layered ultrastructure of the diamond-like 3-D photonic crystals (B: magnification = 6.5k×, scale = 10 µm; C: 15.0k×, scale = 2 µm; D: 64.9k×, scale = 1 µm). Optical images showing the baseline color spectrum of the sensors (E) macroscopically, and (F–G) using light microscopy (F: 10×, scale = 1.0 mm; G: 1000×, scale = 5 µm; two different photonic crystals in F and G).

BID was exposed to repeated insults, the colorimetric properties were not altered until an exposure threshold was surpassed (Fig. 5). These findings demonstrate the durability of the crystalline structure when exposed to low intensity stimuli, and support the possibility to register cumulative responses. Although the pathological responses to repeated blast exposure are unclear, the occurrence of repetitive mild TBI due to impact/inertial loading has been suggested to increase the susceptibility for a more severe outcome in response to a reduced insult (i.e. decreased injury thresholds) (Erlanger et al., 1999; Cantu, 2003; Guskiewicz et al., 2003; Mori et al., 2006). Moreover, there is a link between conventional TBI and increased risk for later development of progressive dementing disorders such as Alzheimer's disease (Tokuda et al., 1991; Nemetz et al., 1999; Guo et al., 2000; Jordan, 2000; Plassman et al., 2000; Jellinger et al., 2001; Smith et al., 2003; Guskiewicz et al., 2005; McMurtray et al., 2006); however, the relevance of this following TBI due to blast is currently unknown.

Mechanisms of blast-induced color change

Following blast exposure, the ultrastructural mechanisms underlying BID color change and loss was evaluated by scanning electron microscopy (SEM). Color change or diminished color correlated with regions exhibiting nanostructural alterations while color loss correlated with regions exhibiting stark microstructural alterations (Fig. 6). On the nano-scale, these alterations consisted of breakage of the material around the pores (effectively opening up the pore size) and collapse of the columns between layers. In some cases, this resulted in layer-by-layer fracture that correlated with loss of color. Higher intensity overpressure resulted in complete layer failure, in some cases revealing the base substrate. There were indications of cleavage fracture habit planes — denoted as (111) in the case of diamond-like structures as shown in Fig. 6, which would be useful in predicting and exploiting mechanical failure on a micro-scale. In addition, color change in some regions was also correlated with decreased pore size or completely fused pores. We suspect that pore contraction may occur directly due to blast-associated thermal effects or indirectly by heat generated from blast-induced acoustic effects (i.e. vibrations) in the materials. Thus, excessive local temperatures could result in melting and/or oxidation of the originally highly structured materials. This mechanism of color change occurred side-by-side with breakage in the horizontal plane or cleavage in the vertical plane. Further investigation of the mechanical behaviors of 3-D photonic crystals under different blast conditions will be directly relevant to exploiting BID color change due to blast. Based on this information, photonic
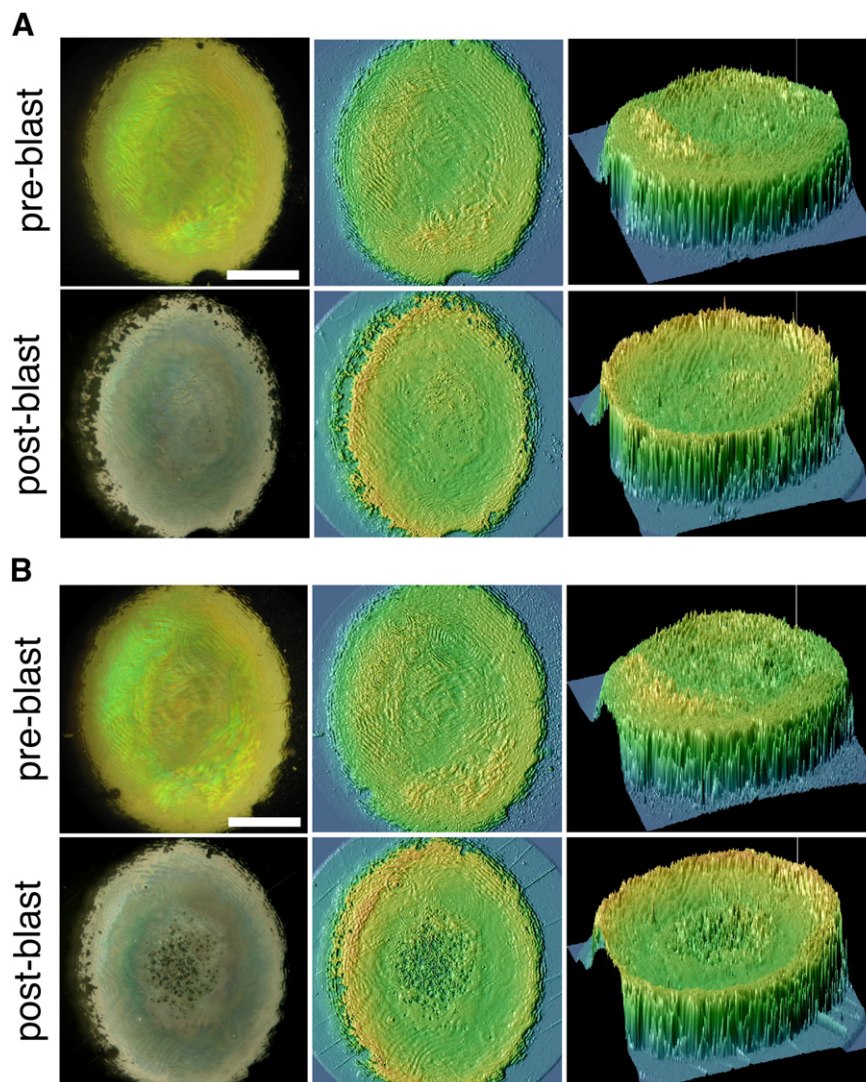
Fig. 3. Color changes following single-pulse overpressure exposure. BID before (top) and immediately following (bottom) exposure to dynamic overpressure, i.e. "blast", at (A) 320 kW/m^2 or (B) 960 kW/m^2 intensity. Images were generated via light microscopy (10×) (left) with corresponding colorimetric surface plots generated using ImagePro Plus (top view: middle; rotated view: right). (A) Exposure intensity of 320 kW/m^2 resulted in a decrease in color throughout and loss of material at edges. (B) Exposure intensity of 960 kW/m^2 resulted in a similar decrease in color and material loss at edges, with additional material loss in the center (note the complete absence of color). Thus, there was a marked change in surface color contours following overpressure exposure at these intensities, and an increase in surface damage with increased exposure. Scale bars = 1.0 mm.

crystalline microstructures may be designed with specific structural characteristics (e.g., pore size, symmetry, and periodicity) and thermal and mechanical properties (e.g., yield strength, Young's modulus, and time–temperature dependence) to tailor the color change in response to specific blast regimes. Thus, tunable structural and mechanical properties will inherently influence the range of shockwaves that are maximally destructive and the degree and mode of failure.

This BID addresses an unmet need for an inexpensive, portable, and lightweight sensor to register the severity of blast exposure. Large populations of warfighters who display either no overt symptoms or more subtle cognitive deficits after blast exposure may nonetheless have suffered physical brain damage (Ling, 2008; Martin et al., 2008). These warfighters typically remain in service, potentially being overlooked for diagnostic testing, resulting in late or no detection and intervention. There is now compelling evidence that many of these warfighters returning from theater have sustained mild TBI, with persisting cognitive and/or psychological symptoms that may prevent their full reintegration into society (Warden, 2006; Martin et al., 2008). Diagnosis of mild TBI is challenging even under controlled circumstances, as subtle or slowly progressive damage to

brain tissue occurs in a manner undetectable by conventional medical imaging. Additionally, there is debate whether mild bTBI symptoms are confused with post-traumatic stress disorder (Hoge et al., 2008; Schneiderman et al., 2008). These factors underscore the need for an objective measure of blast exposure to ensure patients are appropriately stratified to receive proper care.

Conclusions

We have engineered a sensor for blast injury detection that exploits blast-induced optical changes in a photonic crystalline material. Specifically, we demonstrated that blast exposure induced alterations in the 3-D photonic crystalline ultrastructure. These alterations consisted of pore contraction or fusion as well as loss of local material with graded, layer-by-layer failure. The extent of these ultrastructural modifications correlated with color change and/or color loss. These findings demonstrate the ability of a 3-D photonic crystalline material to respond to blast energy by altering structural properties at the nano-scale, creating color changes at the macro-scale. Importantly, these changes in optical characteristics and ultrastructure occurred as a function of blast pressure wave characteristics, suggesting that physical
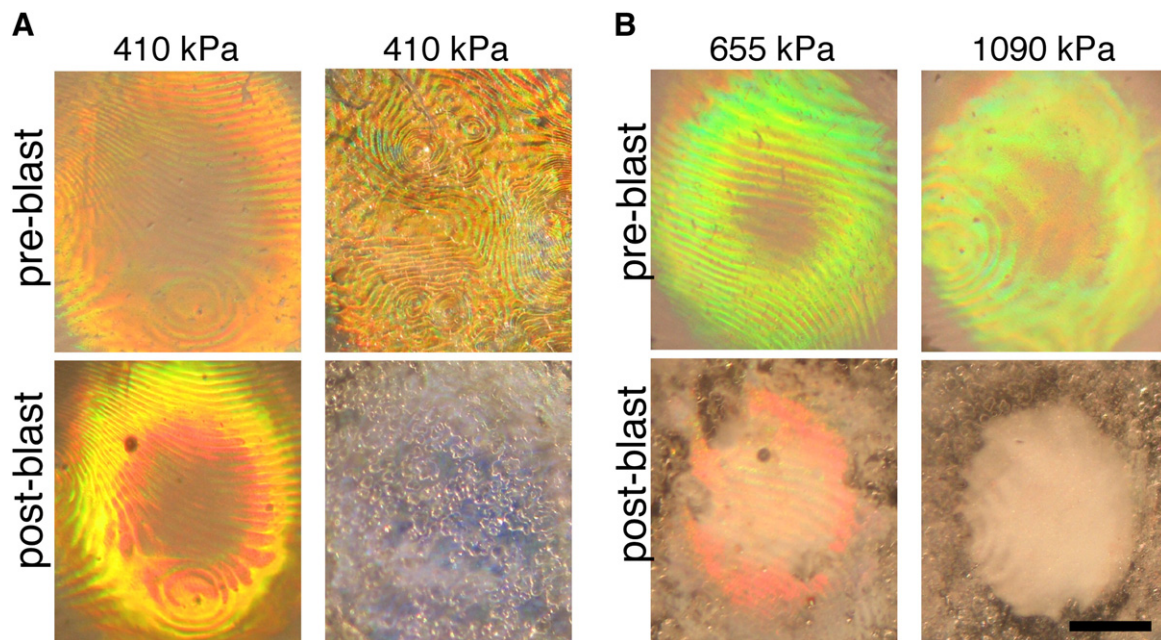
Fig. 4. Color changes and loss following blast exposure. BID with various structural and colorimetric properties were exposed to blast using an explosive shocktube. This surrogate blast model replicates key components of true blast, including rapid shockwave with relatively protracted overpressure/underpressure phases. (A) BID before (top) and after (bottom) blast exposure at a peak overpressure of 410 kPa, which resulted in clear color changes. This demonstrates our ability to engineer BID with distinct color changes even following the same levels of blast exposure. (B) BID before (top) and after (bottom) blast exposure at increased levels, approximately 655 kPa (left) and 1090 kPa (right). There was a clear color change in the BID and potentially material loss. Scale bar = 500 µm.

properties may be tuned to provide dose-dependent responses. By denoting blast exposure beyond pre-calibrated thresholds and making cumulative measurements of blast exposure, this technology may serve multiple purposes: (1) a *diagnostic marker* to enhance medical management of our warfighters; (2) an *investigative tool* to improve our understanding of mechanisms and thresholds for brain injury; and (3) a *design tool* to provide an inexpensive yet sensitive way to assess the performance of blast-mitigation strategies (e.g. helmets, body armor, building safety).

Here, we have demonstrated the efficacy of our material-based strategy using surrogate models of blast exposure. However, several long-term challenges remain before this technology can have widespread implementation. For example, arrays of multiple photonic crystalline microstructures will be developed in order to achieve unambiguous color change/loss for a range of single as well as cumulative blast exposure levels. In addition, live-fire field-testing using conventional explosives will be used to further validate this approach and to refine design specifications. Moreover, it will be
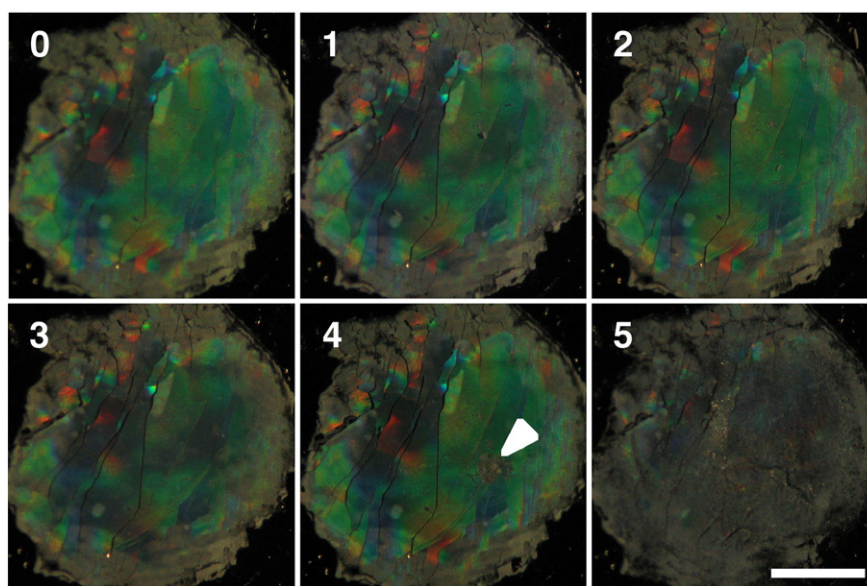
Fig. 5. Colorimetric changes in response to repeated exposure. BIDs were exposed to repeated insults at intensities increasing over three orders of magnitude (0: baseline; 1–5 repeated insults). Lower level exposure did not induce color change (1–2). Repeated exposure induced focal color loss (4, white arrowhead), followed by a nearly complete loss of color (5). Thus, lower intensity overpressure did not alter the colorimetric profile, indicating BID durability. In addition, this suggests that the BID may be tuned to provide dose-dependent responses. Scale bar = 500 µm.
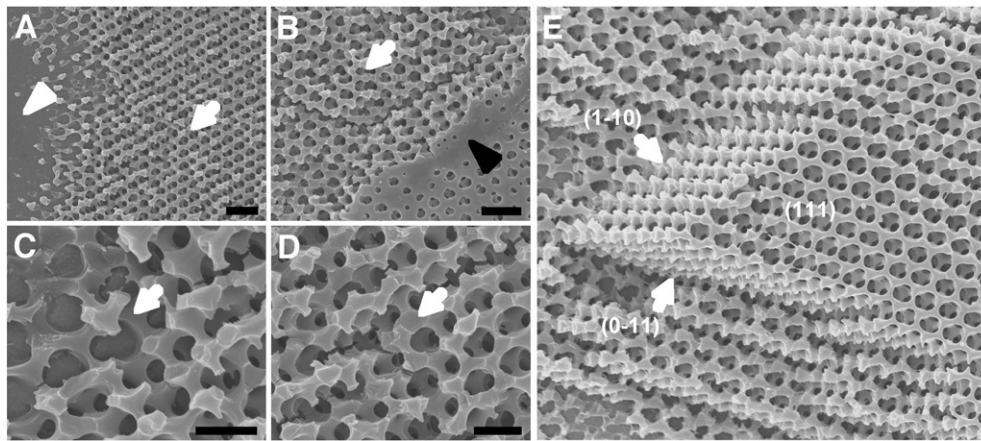
Fig. 6. Ultrastructural changes in response to blast exposure. Scanning electron micrographs demonstrating ultrastructural changes in the photonic crystalline microstructures following high intensity dynamic overpressure exposure. (A) Complete material failure and loss, revealing the base substrate, potentially indicated local regions of high intensity pressure application (white arrowhead) (magnification = 15.0k×, scale = 2 μm). (B) Focal defects were observed adjacent to the original material surface (black arrowhead), which demonstrated a fusion or contraction of the pores in some cases (20.0k×, scale = 2 μm). (C–D) Layer-by-layer failure was observed resulting from column breaks within layers, with, in some cases, maintenance of several residual layers (white arrows) (C: 65.0k×, scale = 1 μm; C: 50.0k×, scale = 1 μm). (E) Demonstration of preferential cleavage along specific planes following rapid overpressure exposure (with planes denoted). Overall, exposure to extremely rapid, high pressure fluctuations resulted in graded, layer-by-layer failure consisting of columnar collapse and layer erosion and/or pore fusion at the surface.

critical to calibrate the BID colorimetric response to specific blast levels (i.e., pressure–time parameters) that induce a range of bTBI severities. Thus, BID structural/colorimetric changes will be correlated with neurocognitive and/or histopathological indications of even mild TBI. Finally, the BID must be implemented in an in-field pilot study, possibly using soldiers serving in active combat arenas. This will allow calibration of color change with the severity of bTBI on an individual basis based on clinical assessment.

Acknowledgments

References

Bauman, R.A., Ling, G.S., Tong, L., Januszkiewicz, A., Agoston, D., Delanerolle, N., Kim, J., Ritzel, D., Bell, R., Ecklund, J.M., Armonda, R., Bandak, F., Parks, S., 2009. An introductory characterization of a combat-casualty-care relevant swine model of closed head injury resulting from exposure to explosive blast. J. Neurotrauma 26, 841–860.

Campbell, M., Sharp, D.N., Harrison, M.T., Denning, R.G., Turberfield, A.J., 2000. Fabrication of photonic crystals for the visible spectrum by holographic lithography. Nature 404, 53–56.

Cantu, R.C., 2003. Recurrent athletic head injury: risks and when to retire. Clin. Sports Med. 22, 593–603.

Cernak, I., Wang, Z., Jiang, J., Bian, X., Savic, J., 2001. Ultrastructural and functional characteristics of blast injury-induced neurotrauma. J. Trauma 50, 695–706.

Erlanger, D.M., Kutner, K.C., Barth, J.T., Barnes, R., 1999. Neuropsychology of sports-related head injury: Dementia Pugilistica to Post Concussion Syndrome. Clin. Neuropsychol. 13, 193–209.

Guo, Z., Cupples, L.A., Kurz, A., Auerbach, S.H., Volicer, L., Chui, H., Green, R.C., Sadovnick, A.D., Duara, R., DeCarli, C., Johnson, K., Go, R.C., Growdon, J.H., Haines, J.L., Kukull, W.A., Farrer, L.A., 2000. Head injury and the risk of AD in the MIRAGE study. Neurology 54, 1316–1323.

Guskiewicz, K.M., McCrea, M., Marshall, S.W., Cantu, R.C., Randolph, C., Barr, W., Onate, J.A., Kelly, J.P., 2003. Cumulative effects associated with recurrent concussion in collegiate football players: the NCAA Concussion Study. Jama 290, 2549–2555.

Guskiewicz, K.M., Marshall, S.W., Bailes, J., McCrea, M., Cantu, R.C., Randolph, C., Jordan, B.D., 2005. Association between recurrent concussion and late-life cognitive impairment in retired professional football players. Neurosurgery 57, 719–726 discussion 719–726.

Hoge, C.W., McGurk, D., Thomas, J.L., Cox, A.L., Engel, C.C., Castro, C.A., 2008. Mild traumatic brain injury in U.S. soldiers returning from Iraq. N Engl J. Med. 358, 453–463.

Jellinger, K.A., Paulus, W., Wrocklage, C., Litvan, I., 2001. Effects of closed traumatic brain injury and genetic factors on the development of Alzheimer's disease. Eur. J. Neurol. 8, 707–710.

Jordan, B.D., 2000. Chronic traumatic brain injury associated with boxing. Semin. Neurol. 20, 179–185.

Kato, K., Fujimura, M., Nakagawa, A., Saito, A., Ohki, T., Takayama, K., Tominaga, T., 2007. Pressure-dependent effect of shock waves on rat brain: induction of neuronal apoptosis mediated by a caspase-dependent pathway. J. Neurosurg. 106, 667–676.

Lee, K.Y., Rishton, S.A., Chang, T.H.P., 1994. High-aspect-ratio aligned multilayer microstructure fabrication. J. Vac. Sci. Technol., B 12, 3425–3430.

Ling, G., 2008. Traumatic brain injury and the global war on terror. The 26th Annual National Neurotrauma Symposium Orlando, FL.

Lorenz, H., Despont, M., Fahrni, N., LaBianca, N., Renaud, P., Vettiger, P., 1997. SU-8: a low-cost negative resist for MEMS. J. Micromech. Microeng. 7, 121–124.

Loubeau, A., Sparrow, V.W., Pater, L.L., Wright, W.M., 2006. High-frequency measurements of blast wave propagation. J. Acoust. Soc. Am. 120, EL29–EL35.

Martin, E.M., Lu, W.C., Helmick, K., French, L., Warden, D.L., 2008. Traumatic brain injuries sustained in the Afghanistan and Iraq wars. J. Trauma Nurs. 15, 94–99 quiz 100–101.

McMurtray, A., Clark, D.G., Christine, D., Mendez, M.F., 2006. Early-onset dementia: frequency and causes compared to late-onset dementia. Dement. Geriatr. Cogn. Disord. 21, 59–64.

Miklyaev, Y.V., Meisel, D.C., Blanco, A., von Freymann, G., Busch, K., Koch, W., Enkrich, C., Deubel, M., Wegener, M., 2003. Three-dimensional face-centered-cubic photonic crystal templates by laser holography: fabrication, optical characterization, and band-structure calculations. Appl. Phys. Lett. 82, 1284–1286.

Moochhala, S.M., Md, S., Lu, J., Teng, C.H., Greengrass, C., 2004. Neuroprotective role of aminoguanidine in behavioral changes after blast injury. J. Trauma 56, 393–403.

Moon, J.H., Yang, S., 2005. Creating three-dimensional polymeric microstructures by multi-beam interference lithography. J. Macromol. Sci., Polym. Rev. C45, 351–373.

Moon, J.H., Ford, J., Yang, S., 2006. Fabricating three-dimensional polymer photonic structures by multi-beam interference lithography. Polym. Adv. Technol. 17, 83–93.

Mori, T., Katayama, Y., Kawamata, T., 2006. Acute hemispheric swelling associated with thin subdural hematomas: pathophysiology of repetitive head injury in sports. Acta Neurochir. Suppl. 96, 40–43.

Nemetz, P.N., Leibson, C., Naessens, J.M., Beard, M., Kokmen, E., Annegers, J.F., Kurland, L.T., 1999. Traumatic brain injury and time to onset of Alzheimer's disease: a population-based study. Am. J. Epidemiol. 149, 32–40.

Okie, S., 2005. Traumatic brain injury in the war zone. N Engl J. Med. 352, 2043–2047.

Plassman, B.L., Havlik, R.J., Steffens, D.C., Helms, M.J., Newman, T.N., Drosdick, D., Phillips, C., Gau, B.A., Welsh-Bohmer, K.A., Burke, J.R., Guralnik, J.M., Breitner, J.C., 2000. Documented head injury in early adulthood and risk of Alzheimer's disease and other dementias. Neurology 55, 1158–1166.

Ribeiro, J.C., Minas, G., Turmezei, P., Wolffenbuttel, R.F., Correia, J.H., 2005. A SU-8 fluidic microsystem for biological fluids analysis. Sensors Actuators Phys. 123–24, 77–81.

Saljo, A., Arrhen, F., Bolouri, H., Mayorga, M., Hamberger, A., 2009. Neuropathology and pressure in the pig brain resulting from low-impulse noise exposure. J. Neurotrauma 25, 1397–1406.

Schneiderman, A.I., Braver, E.R., Kang, H.K., 2008. Understanding sequelae of injury mechanisms and mild traumatic brain injury incurred during the conflicts in Iraq and Afghanistan: persistent postconcussive symptoms and posttraumatic stress disorder. Am. J. Epidemiol. 167, 1446–1452.

Smith, D.H., Chen, X.H., Iwata, A., Graham, D.I., 2003. Amyloid beta accumulation in axons after traumatic brain injury in humans. J. Neurosurg. 98, 1072–1077.

Taber, K.H., Warden, D.L., Hurley, R.A., 2006. Blast-related traumatic brain injury: what is known? J. Neuropsychiatry Clin. Neurosci. 18, 141–145.

Tokuda, T., Ikeda, S., Yanagisawa, N., Ihara, Y., Glenner, G.G., 1991. Re-examination of ex-boxers' brains using immunohistochemistry with antibodies to amyloid beta-protein and tau protein. Acta Neuropathol. 82, 280–285.

Warden, D., 2006. Military TBI during the Iraq and Afghanistan wars. J. Head Trauma Rehabil. 21, 398–402.

Warden, D.L., Ryan, L.M., Helmick, K.M., Schwab, K., French, L., Lu, W., Lux, W., Ling, G., Ecklund, J., 2005. War neurotrauma: the Defense and Veterans Brain Injury Center (DVBIC) experience at Walter Reed Army Medical Center (WRAMC). J. Neurotrauma 22, 1178.

Xu, Y., Zhu, X., Dan, Y., Moon, J.H., Chen, V.W., Johnson, A.T., Perry, J.W., Yang, S., 2008. Electrodeposition of three-dimensional titania photonic crystals from holographically patterned microporous polymer templates. Chem. Mat. 20, 1816–1823.

Yang, S., Megens, M., Aizenberg, J., Wiltzius, P., Chaikin, P.M., Russel, W.B., 2002. Creating periodic three-dimensional structures by multibeam interference of visible laser. Chem. Mat. 14, 2831–2833.